HRC-68-3

HERCULES

A STUDY OF THE MECHANISM OF CHEMICAL REACTIVITY OF NITROGEN TETROXIDE WITH TITANIUM ALLOY

Contract No. NAS 8-21207
Control No. DCN 1-7-54-20173 (1F)
The George C. Marshall Space Flight Center
National Aeronautics and Space Administration

FOURTH QUARTERLY REPORT
April 1, 1968 to June 30, 1968

HERCULES RESEARCH CENTER
HERCULES INCORPORATED
WILMINGTON, DELAWARE

A STUDY OF THE MECHANISM OF CHEMICAL REACTIVITY OF NITROGEN TETROXIDE WITH TITANIUM ALLOYS

FOURTH QUARTERLY REPORT
April 1, 1968 to June 30, 1968

Sponsored by
The George C. Marshall Space Flight Center
National Aeronautics and Space Administration
Contract No. NAS8-21207
Control No. DCN 1-7-54-20173 (1F)

Submitted by
Research Center, Hercules Incorporated
Wilmington, Delaware 19899

November 1, 1968

Albert Z. Conner
Project Leader

Alan D. Craig, Manager
Explosives & Chemical Propulsion
Research Division

A STUDY OF THE MECHANISM OF CHEMICAL REACTIVITY OF NITROGEN TETROXIDE WITH TITANIUM ALLOYS

Foreword

This is the fourth quarterly report prepared by the Research Center, Hercules Incorporated, under Contract No. NAS8-21207, Control Number DCN 1-7-54-20173 (1F) for the George C. Marshall Space Flight Center of the National Aeronautics and Space Administration, and covering the period from April 1, 1968 to June 30, 1968. The work was administered under the technical direction of the Propulsion and Vehicle Engineering Laboratory, Materials Division, of the George C. Marshall Space Flight Center with Mr. W. A. Riehl acting as project manager. Scientific personnel that have participated in this program include:

Mr. A. Z. Conner, Project Leader

Dr. J. B. Arots
Mr. A. H. Betley
} Corrosion Studies

Dr. E. J. Forman, Analytical Coordination

Dr. G. A. Ward, NMR Studies

Mr. A. A. Orr, Spectrophotometer Studies

Mr. R. J. Friant, Mass Spectroscopic Studies

Dr. H. L. Young, Sample Preparation

Dr. J. F. G. Clarke, Jr., Gas Chromatography

Mr. Lawrence Haas, X-ray Emission

Mr. A. B. Peet, Optical Emission and Atomic Absorption Spectroscopy

Mr. L. D. Missimer, Metals Analysis

ABSTRACT

During the past quarter, an additional eleven stress corrosion cracking (SCC) tests were performed. The main objective of the majority of these tests was to establish concentration levels of NO and protonated species that might be critical to the occurrence or inhibition of SCC. This work was made possible by the moderately successful scale-up of a laboratory dehydration unit for the production of 1 to 1.5 liters/hour of dried N_2O_4, and was added by a major analytical breakthrough in the measurement and characterization of the protonated species in N_2O_4.

The test data showed a definite interdependency between combined NO and protonated species concentrations with regard to the production of SCC. Dehydrated samples of RR N_2O_4 caused cracking. The addition of 1,600 ppm. of 99% HNO_3 to dehydrated N_2O_4 did not change the cracking behavior. Additions of NO to dehydrated and normal RR N_2O_4 showed that the dehydrated samples required more NO (>500 ppm.) to inhibit SCC than did the normal samples (150-200 ppm.).

The major analytical breakthrough referred to above involves the use of near-infrared spectrophotometry for the characterization and measurement of the various protonated species in N_2O_4. In the spectral region of 1.3-2.0μ, the following absorption bands have been observed and assigned:

1.405	H_2O	OH stretch overtone
1.45	HNO_2	OH stretch overtone
1.47	HNO_3	OH stretch overtone
1.90	H_2O	OH stretch - HOH deformation combination

The 1.405 and 1.90μ bands are characteristic, well-resolved bands. The absorptions at 1.45 and 1.47μ overlap significantly so that it is difficult to detect and/or determine small amounts of HNO_2 in the presence of larger amounts of HNO_3. The use of multicomponent spectrophotometric techniques or computer-based mathematical treatment will be required for complete analysis. For the first time, the direct qualitative and quantitative characterization of the protonated compounds in N_2O_4 appears possible.

Preliminary application of the near-IR method indicates that RR N_2O_4 contains only HNO_3, while G8 N_2O_4 contains H_2O, HNO_2, and HNO_3. The latter equilibrium mixture changes composition when H_2O, NO, or O_2 is added and when the temperature is changed. The method has been calibrated for HNO_3 but not for HNO_2 or H_2O.

Additional work on the determination of dissolved O_2 in N_2O_4 was carried out. A study of potential sources of error revealed significant variability in the use of syringes for low-level O_2 calibration. It was also found that lack of agreement between liquid and gas phase O_2 determinations is very probably due to the system not being in equilibrium.

TABLE OF CONTENTS

LIST OF FIGURES

INTRODUCTION

The specific objectives of this program are as follows:

(1) To develop a standard stress corrosion test capable of assessing the corrosive nature of various types of dinitrogen tetroxide (N_2O_4) on 6 Al 4 V titanium alloy specimens.

(2) To develop methods of analysis capable of detecting and determining significant differences between various types of N_2O_4.

(3) To identify that constituent or component of N_2O_4 which enhances or induces stress corrosion in 6 Al 4 V titanium alloy.

(4) To attempt to establish the possible presence of stress corrosion inhibitors in certain types of N_2O_4 and to determine the concentration levels that are critical regarding their inhibitory action.

This report describes in detail the results of the experimental work performed during the last quarter. It is felt that the specific goals included within the scope of this program have largely been achieved. However, fundamental aspects of the overall problem remain unresolved and tentative conclusions arrived at during the course of this work require additional experimental verification. A summary report covering the entire program will be issued in the near future.

Phase A. Development and Application of a Standard Stress Corrosion Cracking Test

I. Stress Corrosion Cracking Tests

In the Third Quarterly Report (HRC-68-1, January 1 to March 31, 1968), the successful development of a satisfactory stress corrosion cracking test was described and the results of 14 test runs were presented. During the past quarter, an additional 11 SCC tests have been performed. The main objective of the majority of these tests was to establish concentration levels of NO and protonated species that might be critical to the occurrence or inhibition of stress corrosion cracking. This work was made possible by the development of dehydration and add-back techniques that will be described in subsequent sections. A major analytical breakthrough in the measurement and characterization of the protonated species in N_2O_4 by near-infrared spectrophotometry also was an important factor (see Phase B discussion).

In the latest series of tests, the composition of samples of regular and dehydrated RR N_2O_4 was adjusted by the addition of various amounts of NO, H_2O, 99% HNO_3, and G8 N_2O_4. The results of these tests are summarized in Table 1. Runs 15, 19, 20, and 21 represent an attempt to hold the concentration of protonated species at a low constant level while varying the NO content. The test results indicated that the critical level of NO for SCC inhibition in "dried" N_2O_4 was probably about 500 ppm.

The experimental objectives of the remaining test runs were as follows:

Run 16 - Attempt to prepare and test N_2O_4 with a normal proton level, minimum NO, and no dissolved oxygen.

Run 17 - Attempt to check cracking behavior of N_2O_4-HNO_3 mixture.

Run 18 - Check SCC after addition of water to "dried" N_2O_4 at less than normal level.

Run 23 - Check of inhibitory effect of addition of small amount of water to RR N_2O_4.

Run 24 - Check effect of preliminary contact of U-bend specimens with RNR N_2O_4 followed by reduction of NO level by oxygen addition prior to SCC test.

Run 25 - Attempt to produce sample with normal proton level and less than 200 ppm. NO.

Run 22 - See explanation in Table 1.

It is of particular interest to compare the results of Runs 15 and 21 with those from Runs 24 and 25. In the first pair of tests, all specimens cracked at NO concentrations of 120 and 255 ppm. when the HNO_3 levels were 245 and about 223 ppm., respectively. In the second pair of tests, no specimens cracked at comparably low NO concentrations (175 and 160 ppm.) when the HNO_3 levels were much higher (5,000 and 8,500 ppm.). Runs 16 and 17 showed that about 20-60 ppm. NO is insufficient to provide specimen protection at relatively high HNO_3 levels (5,950 and 1,680 ppm.). These data thus demonstrate a definite interdependency between combined NO and protonated species concentrations with regard to

Table 1

Stress Corrosion Cracking Test

Effect of NO and HNO_3

Run Number	Run Description	NO, ppm. Before Exp.	NO, ppm. After Exp.	HNO_3(1), ppm. Before Exp.	HNO_3(1), ppm. After Exp.	Failure Rate	Exp. Time, Hrs.	Temp. °F.
15	RR Dried, NO as produced in drying	120	122	245	280	10/10	69	162
21	RR Dried, NO as produced in drying	255	200	470(3)	223	10/10	72	166
19	RR Dried + NO	535	485	285	200	0/10	67	162
20	RR Dried + NO	740	720	420	495	0/10	66.5	162
17	RR Dried + 99+% HNO_3	26	55	1,680(2)	1,570	10/10	64	162
18	RR Dried + H_2O	675	670	3,250(2)	2,850	0/10	73	162
16	RR + G8 Blend	36	44	5,950(2)	6,020	10/10	72	162
25	RR + NO	175	140	5,000	5,000	0/10	70	170
23	RR + H_2O	580	560	6,900	6,300	0/10	66.5	170
24	U-bends given 1-hour soak in N_2O_4 containing 535 ppm. NO and 8,500 ppm. HNO_3. O_2 then added to reduce NO level before SCC test.	160	100	8,500	8,900	0/10	68	170
22(4)	RR Dried + NO	292	275	515	435	0/10	48	47-72

(1) Determined by near IR at 1.47μ except as noted. Values should be considered as maximum because of a small interfering peak at 1.48μ whose contribution at the measuring wavelength cannot be estimated with accuracy. See Phase B discussion.

(2) Total proton content determined by NMR and calculated as HNO_3.

(3) Sample believed to be contaminated prior to analysis.

(4) This run was to provide an NO level between Run 19 and 21 at 165°F. but the oven was inadvertently turned off after the run was started.

the production of stress corrosion cracking. Further elucidation of this interdependency will probably require a statistically designed, quantitative study of the composition of the protonated species in equilibrium with the N_2O_4-NO-H_2O system.

Titanium U-bend racks, made from the same sheet used for U-bends, also have undergone SCC at regions of high stress. A leg broke off one rack and cracks are present in other legs of all three racks. Cracks are also present at the bolt rests, at the tensile surface where the strip was sheared, and at the spot-weld areas where the legs are attached to the rack spine. In sharp contrast to the general deterioration of the racks is the acceptable appearance of the 6 Al 4V titanium bolts used for U-bend stressing. None of the twenty, 1/4-inch bolts have identifiable stress corrosion cracks after exposure for 400 and 440 hours in various runs with N_2O_4 compositions that have produced cracks in U-bends. Of course, these bolts differ from the U-bends in configuration as well as in several other ways. For example, they are made from regular grade 6 Al 4V titanium alloy rather than ELI material. In addition, the bolts are loaded at <10% of the average stress in the U-bend although at the thread notches this could be 3 to 5 times higher. The satisfactory behavior of the bolt material emphasizes the fact that compositional, conformational, and stress level factors cannot be ignored in considering the overall stress corrosion cracking problem.

II. Dehydration of N_2O_4

The "dehydration" or reduction of the proton level in RR N_2O_4 was essential to the NO-H_2O study described in the previous section. Early laboratory work showed that the passage of RR N_2O_4 vapors through a column filled with activated Linde Molecular Sieve Type 3A followed by condensation at 0°C. could produce liquid N_2O_4 containing some NO but greatly reduced in proton concentration. This basic procedure was scaled up in a unit capable of producing approximately 1 to 1.5 liters/hour of "dehydrated" N_2O_4. During this same period, near-infrared analytical work showed that HNO_3 is essentially the only protonated compound present in RR N_2O_4. Therefore, using this measurement of HNO_3 as an index of "dehydration", it was found that approximately 95% of the protonated species could be removed in this unit. Starting material containing about 6,000 ppm. HNO_3 was routinely reduced to below 500 ppm. and usually below 300 ppm. Considering the fact that the current system involves transfers from the dry N_2O_4 receiver to SCC test cells and/or sample bulbs under ambient high-humidity conditions, these results are considered to be highly satisfactory. However, it is believed that substantially lower values could be achieved by system modification and humidity control.

Capacity of the 3A Molecular Sieve for the "dehydration" of N_2O_4 has not been determined accurately. However, preliminary estimates are of the order of 2 ml. $N_2O_4/cm.^3$ Molecular Sieve based on 55% vaporization of the charge. At lower initial HNO_3 levels, or with multipass drying, the capacity should be

considerably greater. Lower initial HNO_3 levels should be achievable by rectification through 5-10 theoretical plates at moderate reflux ratios prior to passage through the adsorbent. The use of other types of adsorbents may also be indicated. Since the protonated material to be removed is primarily HNO_3, activated alumina or other types of Molecular Sieve may offer some advantages.

In all instances in which N_2O_4 was passed through an activated Molecular Sieve column, a small amount of nitric oxide was produced. Often the initial N_2O_4 condensate was green, indicating an NO content of >1,000 ppm. The source of the NO is probably from reaction of NO_2 with tightly bound water in the sieve crystal or with adsorbed water incompletely removed by the activation process. Nitric oxide may also be generated by reaction of HNO_3 with the basic sieve material to form water which will then react with additional NO_2. In cases when it is desired to produce a "dry", NO-free sample, the NO (N_2O_3) must be removed by reaction with gaseous oxygen.

An additional dimension of purification is provided by the Molecular Sieve "dehydration" procedure. It was found that the trace metals content of N_2O_4 was significantly reduced by this process. For example, the iron content of a typical sample of RR N_2O_4 was reduced from 0.3 ppm. to about 0.04 ppm. Fe.

III. Add-Back Techniques

Hypodermic syringe techniques were used for the seven add-back experiments reported here. By this approach, for example, 1,400 cc. of NO was transferred, in 100cc. portions, through a silicone rubber septum into one corrosion test cell with minimal water contamination. In other experiments, NO as well as H_2O and O_2 have been added to test cells. The septums are usable for two days when in contact with N_2O_4 vapors at ambient temperatures. After this period they begin to harden and crack and lose ability to seal against the hypodermic needles. In liquid N_2O_4 they do not last much longer than ten minutes. Because of the marginal utility of silicone rubber, other more resistant rubbers, e.g., Viton or other fluorocarbon elastomer, should be tested for this application.

IV. Test Cell Performance

The current test cell design has been used in 23 runs without leakage. Connections are made and broken at least six times on either end of the test cell in the course of each run. Care in handling the cell as well as the design of the end closures have produced a reliable and safe vessel. The cell is not exceptionally robust because it is made of glass and has relatively fragile Teflon tubing protrusions to which needle valves are connected. The valves twist, flex, and turn, but thus far, the seal at the Swagelock fitting has not leaked.

Phase B. Characterization of Propellant N_2O_4

I. Determination of Protonated Species

A. Near-Infrared Spectrophotometry

The NMR method for determination of the total protons in N_2O_4 has two basic deficiencies. First of all, the sensitivity is not very high (50-100 ppm. as H_2O), and secondly the distribution of protonated species remains unknown. Attempts to resolve the peaks of the protonated species from each other by operation at subambient temperatures down to -80°C. have thus far failed. The lack of promise of the NMR approach, and an early paper(1) on vapor phase near-infrared (NIR) spectra of HNO_3 and HNO_2, led to an investigation of the NIR region of the absorption spectrum as a possible source of information concerning the nature and distribution of the protonated species in N_2O_4.

Preliminary results were very encouraging. Examination of the absorption spectra of liquid N_2O_4 samples in the 1.3-1.6μ region revealed definite differences between RR and G8 N_2O_4. The spectrum of RR N_2O_4, containing about 850 ppm. "water", showed only one characteristic band at 1.47μ. The spectrum of G8 N_2O_4, also containing about 850 ppm. "water", showed the same 1.47μ band, a shoulder at about 1.45μ, and an additional well-resolved band at 1.405μ. Additional scanning of the G8 spectrum revealed the presence of another band at 1.90μ that was not present in RR N_2O_4.

---

(1) E. J. Jones, J. Am. Chem. Soc., 65 2274 (1943).

A sample of RR N_2O_4 was dried by distillation through a column of 3A Molecular Sieve and treated with O_2 to remove traces of NO. Very little absorption was observed in the 1.35μ to 1.55μ region. Addition of a small amount of water to this sample caused the appearance of the 1.405, 1.47, and 1.90μ bands. The presence of the shoulder at 1.45μ could not be established with certainty.

D_2O was added to another sample of the dried RR N_2O_4 and it was observed that the sample turned green but no bands developed in the 1.4-1.5μ region. The 1.405, 1.47, and 1.9μ bands had shifted to 1.89, 1.92 and 2.56μ, respectively, which indicated that all three of these original bands were due to protons and were probably OH stretch overtones of different molecular species. The 1.9μ band observed in wet green N_2O_4 falls where the OH stretch-HOH deformation combination band of H_2O should be, and since no other compound has two hydrogens on a single oxygen, this band is considered to be unique to water. Oxygenation of G8 N_2O_4 simultaneously eliminated the 1.405, 1.45, and 1.9μ bands and enhanced the 1.47μ band. The relative intensities of the 1.405, 1.45, and 1.47μ bands were also found to be temperature dependent (see Figure 1). The 1.47μ band was definitely assigned to HNO_3 by an experiment in which 99% HNO_3 was added to dry N_2O_4. A series of additions of 99% HNO_3 produced a calibration curve suitable for quantitative measurements.

Although the oxygenation experiment suggested that the 1.405μ band was due to HNO_2, additional proof was required. Approximately 0.5 ml. of liquid N_2O_3 was added to about 50 ml.

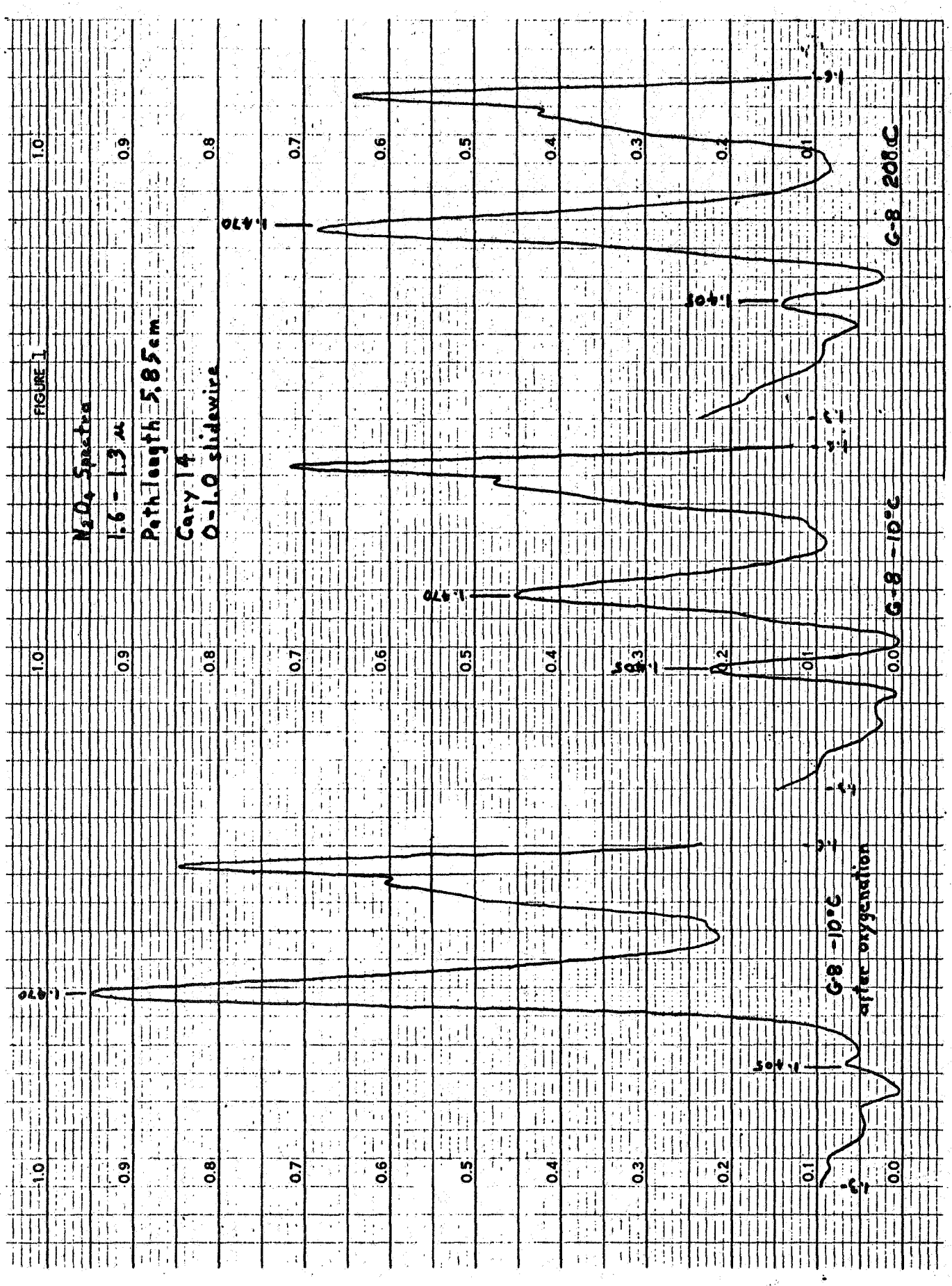
FIGURE 1
N_2O_4 Spectra
1.6 - 1.3 μ
Path length 5.85 cm
Cary 14
0-1.0 slidewire
G-8 20°C
G-8 -10°C
G-8 -10°C
after oxygenation
1.470
1.304
1.470
1.304
1.470
1.304
1.0
0.9
0.8
0.7
0.6
0.5
0.4
0.3
0.2
0.1
0.0

of RR N_2O_4 in a glass bulb, and the resulting mixture scanned. The 1.47μ band decreased and the 1.45μ shoulder and 1.405μ band appeared. Further addition of N_2O_3 caused the 1.45μ shoulder to become a definite band with further decrease of 1.47μ band. With this evidence, it was then suspected that the 1.45μ band might be HNO_2 and that the 1.405μ band might be due to H_2O.

In an attempt to generate HNO_2 under simplified equilibrium conditions, a new approach was tried. A water-saturated sample of CCl_4 was first scanned in a standard 10 cm. cell using the 0-0.2 absorbance slidewire. The NIR spectrum showed two water bands at 1.89μ and 1.395μ(Figure 2) comparable to the 1.90μ and 1.405μ bands observed in G8 N_2O_4. Since N_2O_3 is the anhydride of nitrous acid, addition of N_2O_3 to the wet CCl_4 should generate only HNO_2 at the expense of the water present. A small amount of liquid N_2O_3 was added to the wet CCl_4 and the mixture scanned. The 1.89 and 1.395μ water bands disappeared and a new band at 1.445μ appeared (Figure 3) comparable to the 1.45μ band in N_2O_4. Addition of N_2O_3 to dry CCl_4 showed only a weak 1.45μ band probably due to a small amount of water in the "dry" CCl_4, but definitely showing that the band was not due to N_2O_3 per se (Figure 5). Addition of 99% HNO_3 to dry CCl_4 showed a band at 1.465μ comparable to the 1.47μ band in N_2O_4. An additional experiment in which successive alternate additions of small amounts of liquid N_2O_3 and N_2O_4 to wet CCl_4 showed the 1.445μ band increased and the 1.465μ HNO_3 band decreased with addition of N_2O_3 while the opposite was true for addition of N_2O_4 (Figure 4). The 1.395μ and 1.89μ water bands decreased only slightly through the course of the additions.

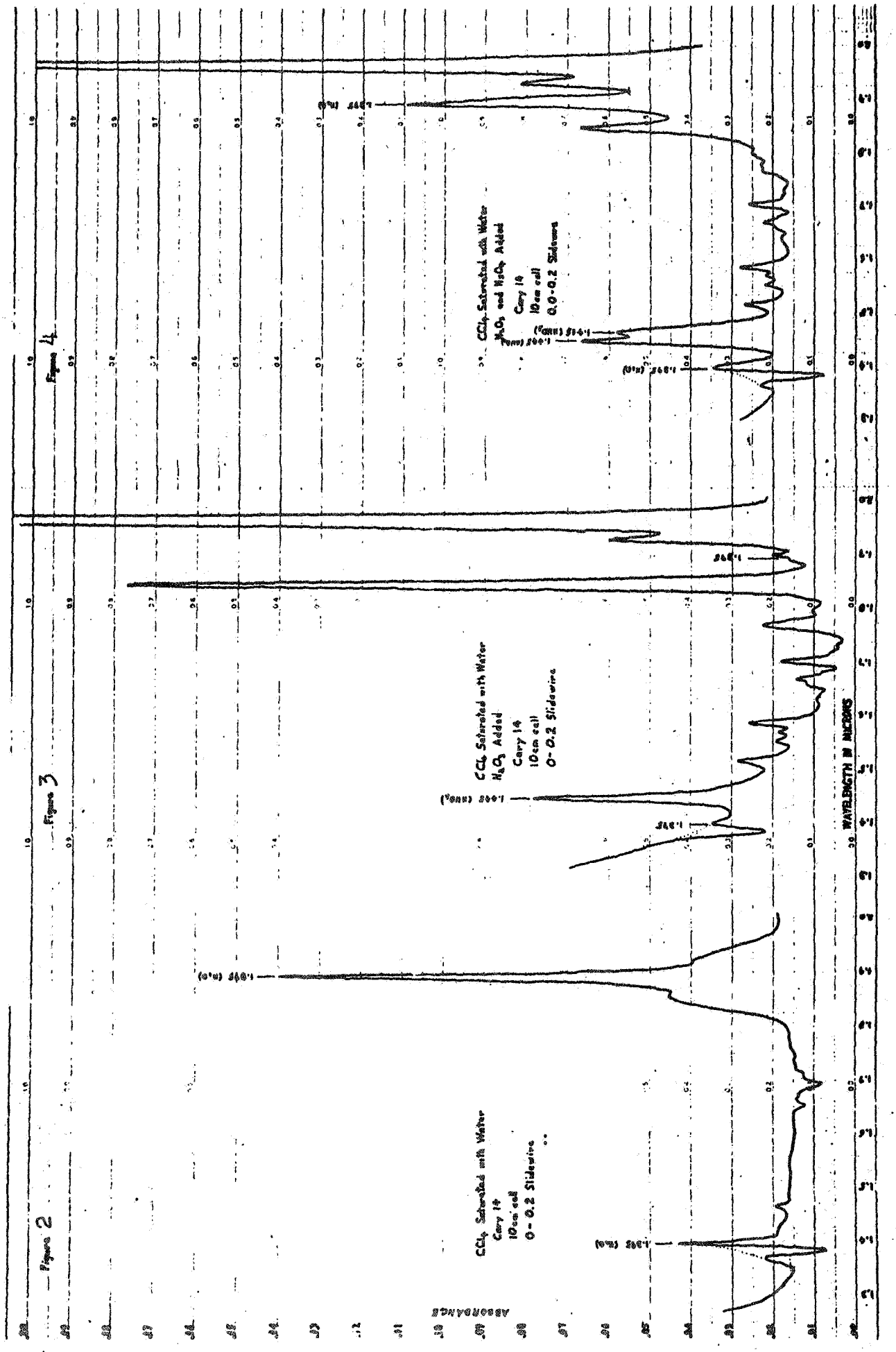
Figure 2
CCl4 Saturated with Water
Cary 14
10cm cell
0 - 0.2 Slidewire
Figure 3
CCl4 Saturated with Water
H2O2 Added
Cary 14
10cm cell
0 - 0.2 Slidewire
Figure 4
CCl4 Saturated with Water
H2O2 and NaOH Added
Cary 14
10cm cell
0.0-0.2 Slidewire
ABSORBANCE
WAVELENGTH IN MICRONS

Figure 5

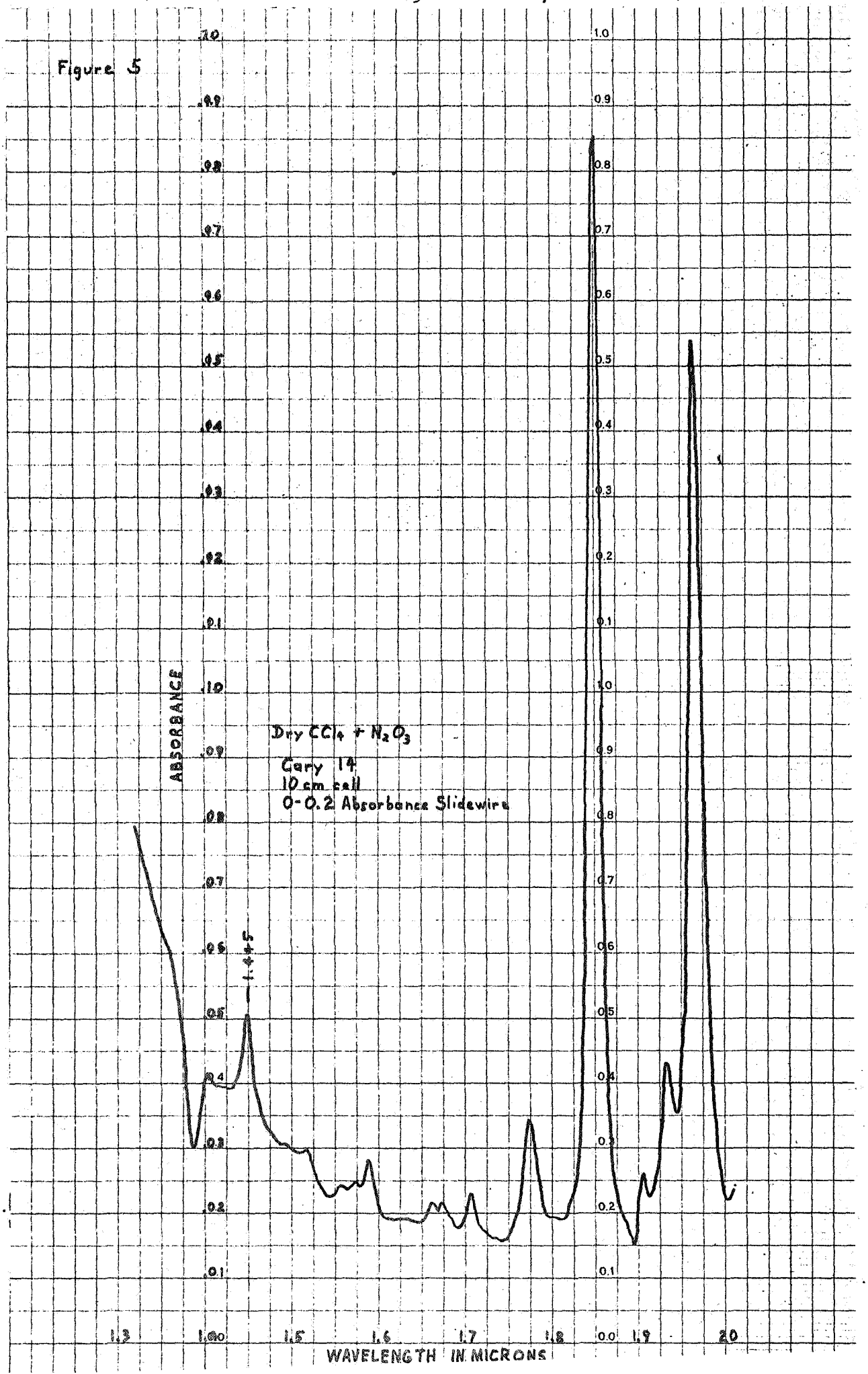
ABSORBANCE
Dry CCl_4 + N_2O_3
Cary 14
10 cm cell
0-0.2 Absorbance Slidewire
1.445
WAVELENGTH IN MICRONS
1.3
1.60
1.5
1.6
1.7
1.8
1.9
2.0

On the basis of the above experiments, the four bands have now been assigned as follows:

1.405μ	H_2O	OH stretch overtone
1.45μ	HNO_2	OH stretch overtone
1.47μ	HNO_3	OH stretch overtone
1.90μ	H_2O	OH stretch-HOH deformation combination

A spectrum of N_2O_4 containing all four bands is shown in Figure 6.

It has been noted that the ratio of the 1.405μ water band and the 1.47μ HNO_3 band in N_2O_4 changes with temperature. This may prove valuable in studying the temperature dependence of the complicated equilibria involved. However, considerable further effort would be required for such studies and to calibrate the bands for quantitative measurement of the different species.

The resolution of the 1.45μ and 1.47μ bands is not very good and it may be necessary to resort to digitization and mathematical resolution of the peaks by computer, or to multi-component spectrophotometric techniques.

Another complicating factor has been encountered in examining the spectra of "dehydrated" red N_2O_4 at high sensitivity (5.85 cm. cell with 0-0.2 absorbance slidewire) for traces of residual protonated compounds. A pair of small bands at about 1.41 and 1.48μ are always present and constitute significant interferences in the quantitative measurement of very low levels of water and HNO_3 (Figure 7). The intensities of these bands appear relatively

Figure 6

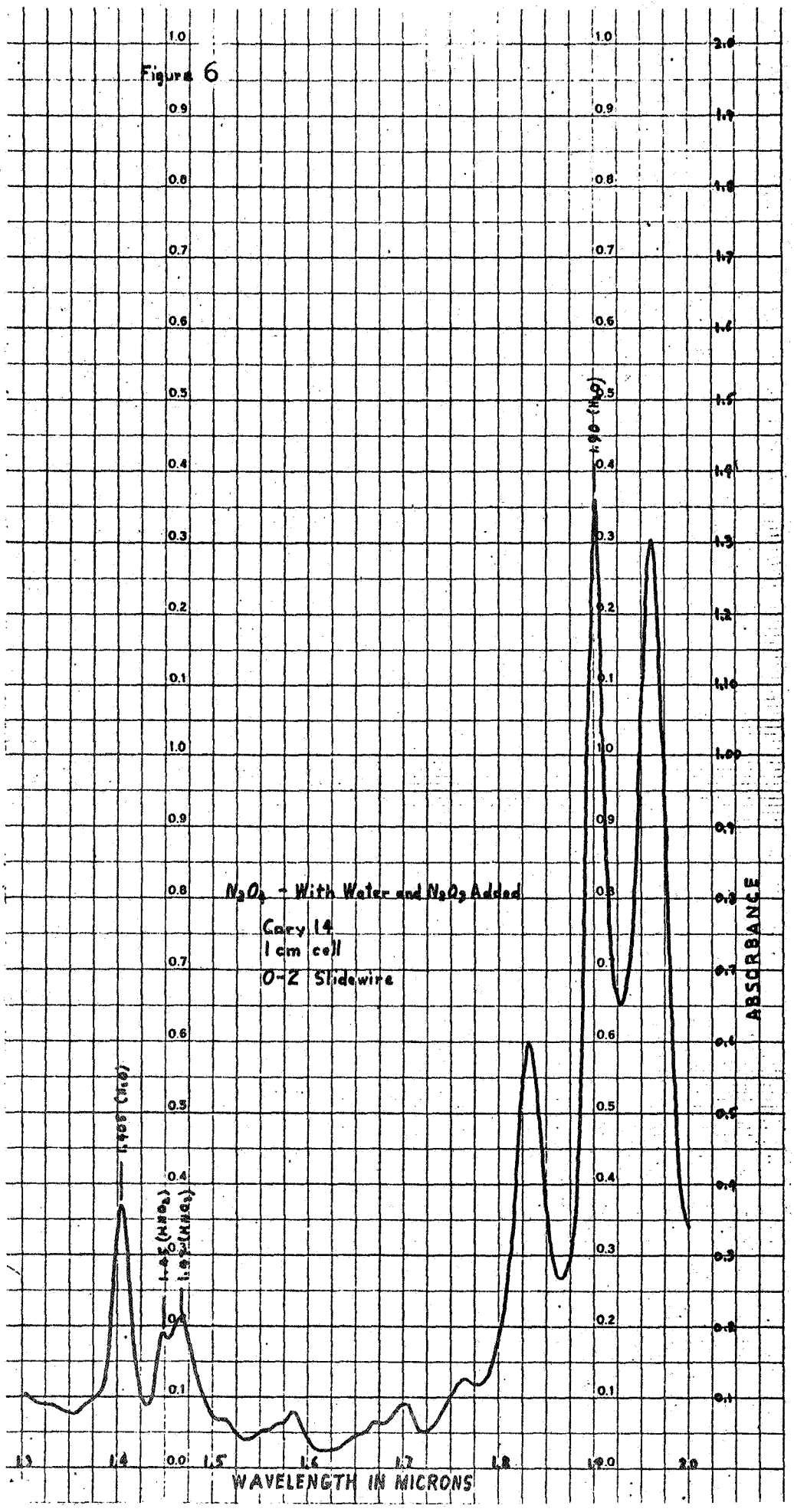
N_2O_4 - With Water and N_2O_3 Added
Cary 14
1 cm cell
0-2 Slidewire
1.44 (HNO3)
1.49 (HNO3)
1.90 (H2O)
ABSORBANCE
WAVELENGTH IN MICRONS

Figure 7

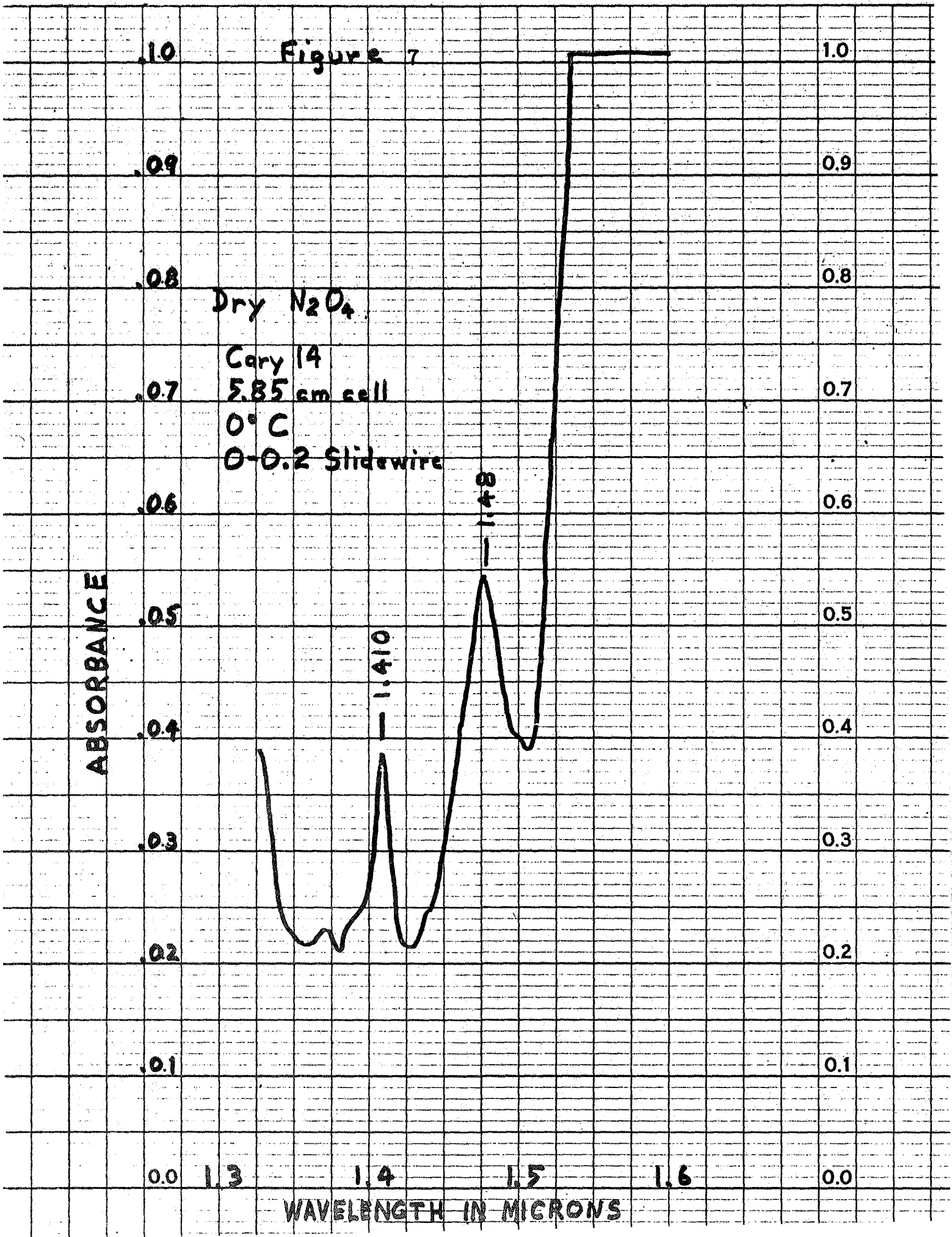
Dry N_2O_4
Cary 14
5.85 cm cell
0° C
0-0.2 Slidewire
1.410
1.585
ABSORBANCE
1.0
.09
.08
.07
.06
.05
.04
.03
.02
.01
0.0
1.3
1.4
1.5
1.6
WAVELENGTH IN MICRONS

constant for a given path length and are not temperature dependent nor affected by oxygen. They probably represent higher overtone or combination bands associated with N_2O_4 itself. The band at 1.48μ interferes with the measurement of HNO_3 at 1.47μ and may contribute a "blank" value equivalent to 100-200 ppm. HNO_3. Until a suitable correction procedure can be worked out, all HNO_3 analyses utilizing this procedure must be reported as maximum values.

All of the near-infrared work was performed on a Cary Model 14 spectrophotometer equipped with a 0-0.2 absorbance, scale expansion slidewire. The cells used were (1) the same temperature controlled cell used for the visible spectrophotometric determination of NO, with NIR-silica windows and a 1 cm. path length, and (2) a special stainless steel, high pressure cell (Figure 8) having a 5.85 cm. path length and fitted with a tubular mixing chamber and a septum for the addition of various compounds.

B. Nuclear Magnetic Resonance

In the Third Quarterly Report, it was reported that solutions of RR N_2O_4 in $CDCl_3$ and CH_2Cl_2 had been studied by NMR at temperatures in the -50° to -60°C. range in an attempt to slow down the proton exchange between the acidic species present and observe separate NMR peaks for each of them. Since that time, NIR studies of the OH stretching absorption bands in N_2O_4 have shown that only HNO_3 is detectable in RR N_2O_4, accounting for the lack of observed NMR line broadening.

The low-temperature experiments were repeated during the past quarter using G8 N_2O_4 in which the presence of more than one type of -OH is shown by NIR. Again, no significant change

FIGURE 8

SPECIAL STAINLESS STEEL CELL
85 CM. PATHLENGTH NIR SILICA WINDOWS

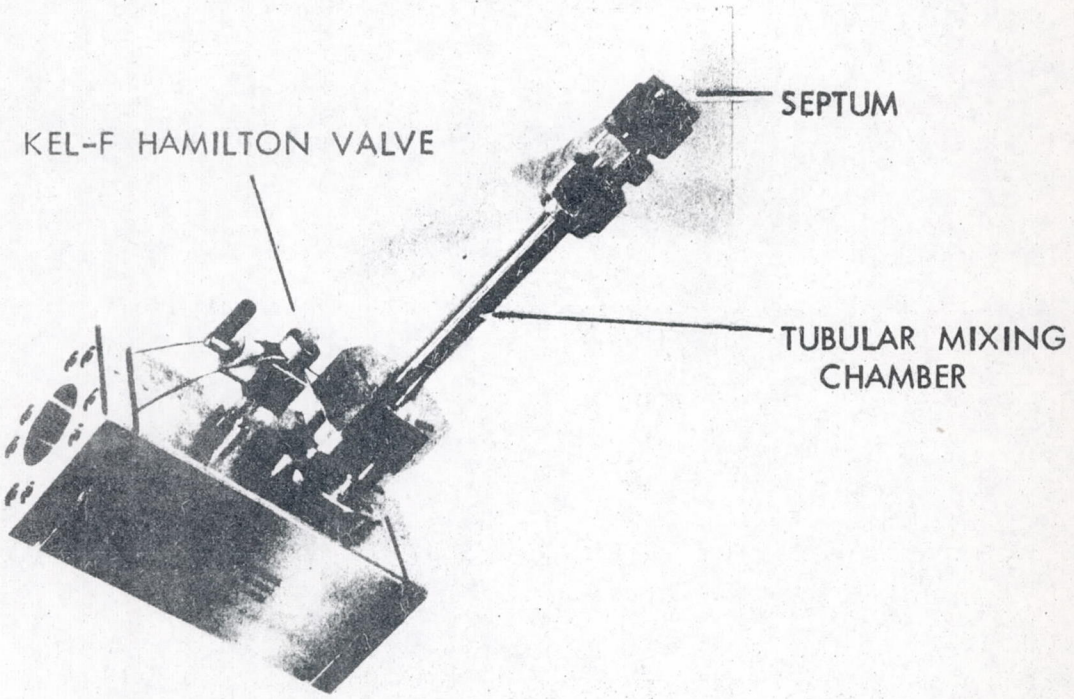

in the shape of the water peak in N_2O_4 was observed as the temperature was decreased. At approximately -45°C. the solubility of protonated species in N_2O_4 had decreased sufficiently that a separate aqueous phase was observed floating on the N_2O_4 and the NMR signal due to dissolved water was barely detectable.

Previous experiments with a model system of 1:1 HNO_3-H_2O in acetone indicated that, if this approach is to succeed, a solvent system would have to be found in which N_2O_4-water mixtures could be studied in homogeneous solution at less than -85°C. Since no such system has been found, work in this area was discontinued.

II. Determination of Oxygen by Gas Chromatography

Work has continued this past quarter on resolving discrepancies in the calibration for oxygen at low levels, and on the further establishment of the relationship between gas and liquid phase analyses through Henry's Law.

The previously reported difficulty (Third Quarterly Report) in obtaining a constant calibration factor at low levels of oxygen (0.3 to 0.8 micrograms) has been traced to an apparent inability to inject accurately known, very small volumes of oxygen (air) into the chromatograph. The use of several different syringes to introduce 1.0 microliter volumes of air was investigated. The data obtained appear in Table 2. Also included are data for 50 microliter aliquots from two types of syringes to show that with larger volumes of air there is little error encountered in using one syringe over another.

Table 2

Variability of Oxygen Calibration Factor

With Type of Syringe Used

Syringe Capacity (Micro-liters)	Micrograms of O_2 Injected	No. of Detns.	Average Response Factor $\mu g./cm.^2$	% Relative Std. Deviation
1.0	0.274	6	0.526	5.2
10.0(a)	0.274	6	0.432	7.9
10.0(a)	0.411	6	0.441	5.5
10.0(a)	0.274	-	-	-
100(b)	13.7	3	0.401	1.2
1000(c)	13.7	3	0.405	2.2

(a) See discussion below.
(b) Hamilton fixed needle liquid syringe.
(c) 1.0 ml. Precision Sampling Gas Syringe.

Differences are quite apparent between types of syringes. The 1.0 microliter syringe yields a larger value for the response factor than does the 10.0 microliter syringe, indicating that a smaller amount of oxygen was injected than calculated from the gas law for a 1.0 microliter volume. The fourth row of Table 2 was added to show what happens when a not obviously loose-fitting plunger of a new 10.0 microliter syringe is encountered - no air was apparently introduced into the chromatograph. The ability of the other 10 microliter syringe to deliver a reproducible quantity of air was due to a fine film of oil on the plunger, which made it fit snugly in the syringe barrel.

Because of these poor calibration results at low oxygen levels, it was decided to extrapolate the linear value obtained at higher levels to levels below 1.0 microgram of oxygen.

Additional work was done to establish the relationship between the gas and liquid phase analysis through application of Henry's law(7). Previous data (Third Quarterly Report) had indicated that concentrations in the liquid phase at low oxygen levels were generally higher when the liquid was assayed directly than would be predicted from analysis of the gas phase. At higher oxygen levels, agreement appeared to be good, but not enough data was available to verify this conclusion.

Oxygen, in varying amounts, was added to a sample of RR N_2O_4 and then both gas and liquid phases analyzed. The oxygen was added to the gas phase with a gas syringe from a 99+% source. The gas and liquid phases were mixed several times by inverting the flask and allowing to stand overnight. The data from these experiments are given in Table 3, and plotted, along with all previous data in Figure 9. As can be seen, the trend of low results as calculated from the gas phase has been, in general, reversed.

The reason for the reversal was not known until an experiment was performed wherein the sample was analyzed after oxygen addition, allowed to stand and then reanalyzed. The data from this experiment (X16300-64) are given as the last three results of Table 3 and are plotted as points A, B, and C on Figure 9.

Table 3

Relationship of Gas Phase Analysis to Liquid

Analysis - Oxygen Add-Back Experiment

Designation	Partial Pressure of Oxygen in the Gas Phase, Atm.	ppm. Oxygen in the Liquid Calculated from P_{O_2} in Gas	No. of Dets.	S	Sr,%	ppm. Oxygen in the Liquid by Direct Analysis	No. of Detns.	S	Sr,%
X16300-44	6.06×10^{-2}	21.4	8	8.0×10^{-3}	13.1	17.2	6	0.5	3.1
X16300-45	6.01×10^{-2}	21.2	6	5.3×10^{-3}	8.8	20.0	6	1.0	5.0
X16300-46	0.116	41.2	6	4.6×10^{-3}	4.0	34.8	6	1.6	4.5
X16300-47(a)	8.52×10^{-3}	3.0	5	5.7×10^{-4}	6.6	2.8	5	0.2	6.8
X16300-56(b)	0.666	235.6	6	2.5×10^{-2}	3.7	205.1	6	7.2	3.5
X16300-57(a)	4.90×10^{-2}	17.3	6	1.8×10^{-3}	3.7	12.7	5	0.9	6.8
X16300-59(a)	4.94×10^{-3}	1.7	5	1.8×10^{-4}	3.7	2.2	5	0.4	15.9
X16300-60	0.0855	30.2	5	1.7×10^{-3}	2.0	27.4	7	1.5	5.5
X16300-61(a)	2.60×10^{-3}	0.9	5	2.7×10^{-4}	10.4	1.5	5	0.1	6.3
X16300-64	5.45×10^{-2}	19.3	6	3.9×10^{-3}	7.2	12.3	5	0.8	6.9
X16300-64R	2.96×10^{-2}	10.5	8	1.6×10^{-3}	5.3	11.8	6	1.1	9.7
X16300-64RR	1.89×10^{-2}	6.7	8	1.1×10^{-3}	5.8	7.6	6	0.7	9.1

(a) After freezing and evacuation of previous sample and standing overnight.

(b) Point not included in Figure 1.

Figure 9

The Determination of Oxygen in N_2O_4 Results Calculated from an Analysis of the Gas Phase Versus Results from the Direct Analysis of the Liquid Phase

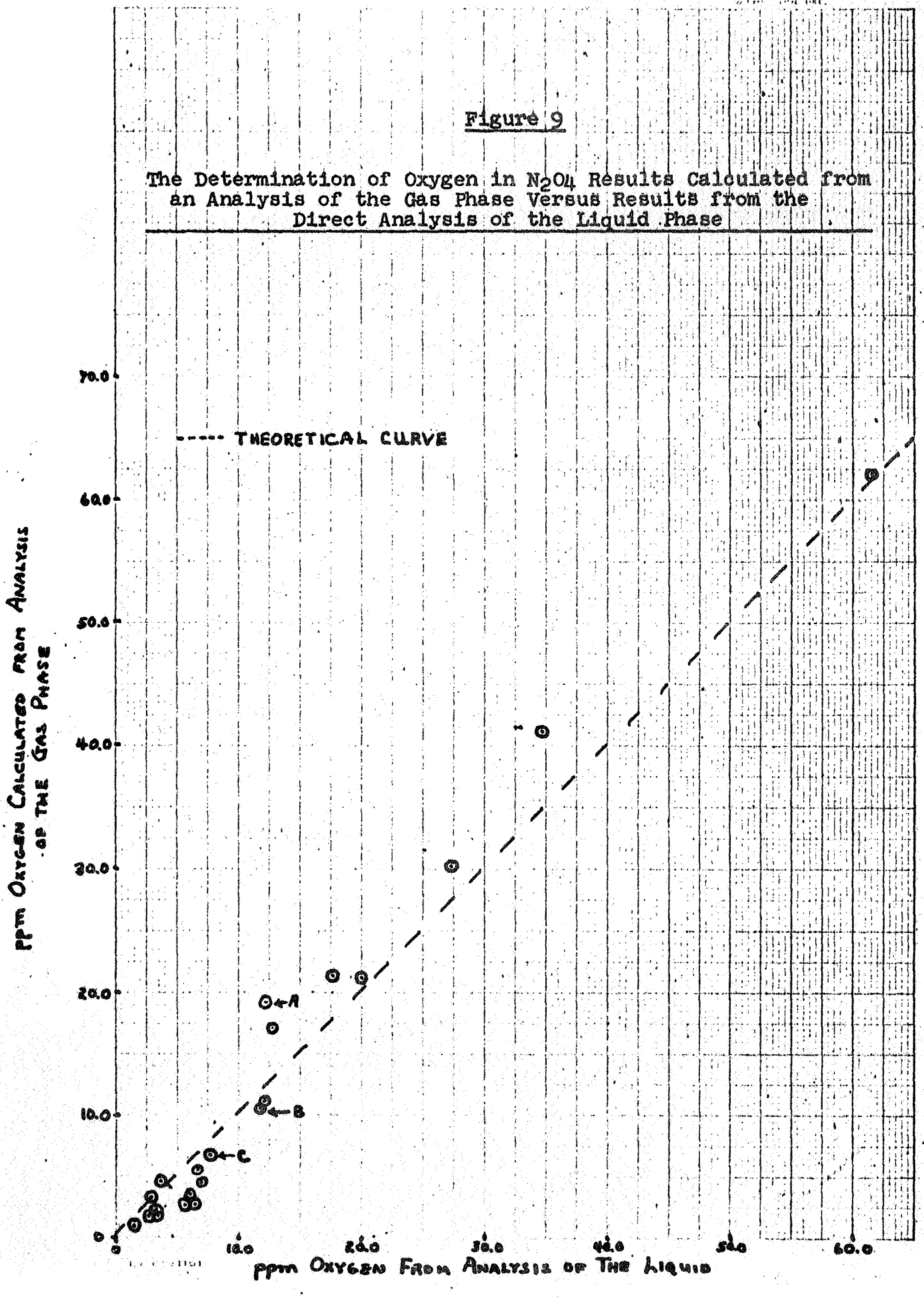

Since point "A" was obtained 2 days after oxygen addition, point "B" 2 days later, and point C some 6 days after oxygen addition, it is apparent when oxygen is added in small amounts to a relatively large gas phase volume, the equilibrium between gas and liquid is established very slowly. Further work should be done on this aspect of the analysis, since it might explain the low results obtained for the liquid when oxygen is removed from the gas phase by freezing and degassing. The largest discrepancies were observed with those samples which had been dried and degassed during experiments to prepare a low level nitric oxide calibration curve. In general, oxygen determinations were made just hours after the degassing process had been carried out. Hence, the oxygen content may have been low in the gas phase for these samples due to nonestablishment of equilibrium.

As a matter of interest, several other gases were run on the Molecular Sieve column used in this work. A summary of the gases and retention data relative to nitrogen on 13X Molecular Sieve are given in Table 4. Of special note is the fact that hydrogen can be readily separated from all the other gases on this column. Aside from changing the carrier gas from helium to nitrogen, no modification of the equipment is necessary for this determination.

Table 4

Relative Retentions of Various Gases On 13X Molecular Sieve Column at 25°C.

Gas	Relative Retention
Hydrogen	0.40
Argon	0.62
Oxygen	0.62
Nitrogen	1.00
Nitric Oxide(a)	~2.0
Carbon Monoxide	2.40
Nitrous Oxide	6.75

(a) Variable, depending on concentration.